COGNITIVE ANTI-JAM RADIO SYSTEM

Raghavendra S. Prabhu, Esteban L. Vallés, Philip A. Dafesh
(Digital Comm. Implementation Dept. The Aerospace Corporation)
Email: raghavendra.prabhu@aero.org

ABSTRACT

Existing Anti-Jam (AJ) and interference mitigation techniques are based on the assumption that the nature of interference is known a priori. Generally, one or more fixed AJ techniques (FATS) are applied to reduce the impact of the jammer or interferer to a receiver. A more general approach is to apply cognitive radio technology, whereby the receiver's AJ processing and receiver signal processing adapt to the incoming interference environment by determining the characteristics of the interference, then jointly optimizing signal processing to mitigate the characterized jammer or interferer. We refer to this approach as a Cognitive AJ Radio System (CARS). The CARS architecture consists of three primary components: a signal analysis block that estimates the characteristics of the signal and jammer, an interference mitigation algorithm that adapts its AJ processing to the measured jammer characteristics, and a receiver signal processing block that adapts to the measured signal and jammer characteristics. This paper compares the performance of a representative CARS architecture to that of a FATS architecture when applied to a direct-sequence spread spectrum (DSSS) receiver. The bit error rate (BER) performance of CARS and FATS under the influence of various types of jammers is evaluated by simulation. Simulation results show that the CARS approach allows data demodulation to be reliably performed even in severe jamming conditions, whereas FATS approaches fail to achieve such performance levels.

1. INTRODUCTION

Interference caused by intentional or unintentional jamming, co-channel users, or adjacent channel users can cause severe degradation in receiver performance. In cognitive radio systems, for example, unintentional jamming occurs when a cognitive user transmits on a channel that was misdetected as being available. Depending on the scenario, various techniques may be applicable, see [1] for a categorization of techniques.

In this paper, we restrict our attention to a single antenna/channel Direct-Sequence Spread Spectrum (DSSS) receiver. Although the inherent processing gain of a DSSS system provides reasonable interference rejection capability, a strong interferer can still render a link unusable [2]. However, depending on the time-frequency nature of the strong interference signal, it may be possible to achieve relatively good performance by applying signal processing techniques at the receiver. Several fixed Anti-Jam (AJ) techniques (FATS), such as filtering and transform domain excision, have been proposed for interference mitigation in a single-channel DSSS system [3], [4]. Some techniques can be more effective than others, depending on which properties of the signal and the interference are assumed to be known [5], [6].

The Discrete Fourier Transform (DFT) is a popular choice for transform domain excision systems [7], [8], [9] primarily due to the low-complexity Fast Fourier Transform (FFT) algorithm. Transform domain excision techniques perform well when the interference signal aligns with as few basis functions as possible. When the interference signal is of a fixed type, it is possible to design transforms that *align* well with the interference and can effectively mitigate it[10]. However, excision systems that use a fixed basis (that do not adapt to the interference) will not be adequate when the interference is dynamic and changing. With the increase in adoption of software radio technology, the interference encountered will only become more challenging. We refer to fixed-basis systems as fixed AJ techniques (FATS), an example of which is the system in [9].

To address the problem of changing interference, adaptive subband transforms have been proposed [11]. However, choosing a non-uniform basis may result in susceptibility to certain types of interference that are not aligned with the subband transform. Recently, [12] suggested an approach that uses the FFT and Fractional FFT (FrFFT), where all possible transform combinations are evaluated in order to compute a metric called *compression gain*. Based on this metric, the best transform is chosen to excise the interference. However, this approach can have a large complexity if there are many transform combinations to evaluate. While these techniques may theoretically mitigate a changing interferer, they require a search over a large space of possible transform combinations, which will fail if the interference is changing more rapidly than the time required to search many jammer hypotheses. Moreover, the complexity of such approaches grows nonlinearly with the number of jammer hypotheses, where each hypothesis consists of a jammer with a particular set of possible characteristics, including time variation, center frequency, amplitude, phase, etc.

In this work, we investigate a novel Cognitive Anti-Jam Receiver System (CARS) approach whereby the AJ signal processing and the receiver signal processing are jointly adapted to more effectively mitigate interference than is possible using FATS approaches. The CARS approach generally

estimates the characteristics of the signal and jammer, and uses these measured characteristics to configure an interference mitigation algorithm that adapts its AJ processing and receiver signal processing to optimize receiver bit error rate and/or synchronization performance. In this case, the parameters of the FFT itself are adapted to the changing interference characteristics through a cognitive process.

In this paper, a representative CARS architecture is employed consisting of an interference estimator using a bank of channelized radiometers, decision logic, a time and time-frequency jammer excision block (based on the FFT algorithm), and a demodulator that is adapted to the measured jammer characteristics [13]. The CARS approach is illustrated using both an ideal *genie* jammer estimator with a priori knowledge of the jammer characteristics and an imperfect estimator based on the channelized radiometers. The AJ system using the genie is referred to as GENIE for convenience. We demonstrate the relative performance of the CARS architecture as compared to conventional FATS approaches when applied to a DSSS receiver. The BER performance of CARS and FATS are simulated under the influence of various jammer types. The CARS estimation algorithm does not assume much about the interference, except that it is sparse in some basis, or not like white noise.

The paper is organized as follows. In section 2, we introduce the signal model (2.1), CARS architecture (2.2) and interference classes (2.3). In section 3 and section 4, we describe the operation of the main components of the CARS architecture, the signal analyzer, and the time/frequency excisor, respectively. In section 5, we present simulation results that demonstrate the performance of the CARS architecture. The paper is concluded in section 6.

2. System Model

2.1. Signal model

At the receiver, a discrete-time complex baseband model is used to describe how a BPSK-modulated signal is affected by AWGN noise and some *type* of interference:

$$\begin{aligned} y(n) &= s(n) + j(n) + w(n) \\ &= \sqrt{\mathrm{SNR}}\, c(n)\, x_l + \sqrt{\mathrm{JSR}}\, j'(n) + w(n) \end{aligned}$$

where s is the transmitted signal, j is the interference, c is the oversampled spreading code normalized to unit power, $x_l = (-1)^{b_l}$ is the BPSK-modulated symbol for the l-th bit period and data bit b_l, j' is interference (jamming) signal normalized to unit power, and $w(n)$ is an i.i.d. zero-mean, unit variance, complex Gaussian noise random variable. The discrete sample indices for a symbol (bit) period T range over $0 \le n \le KN-1$, where K is the number of samples per chip and N is the number of chips in the spreading code. In this work, we will often operate on vector sequences and different transformations of these sequences. We define the power of a sequence, s, as:

$$P_s = \frac{\mathrm{E}||s||^2}{KN}$$

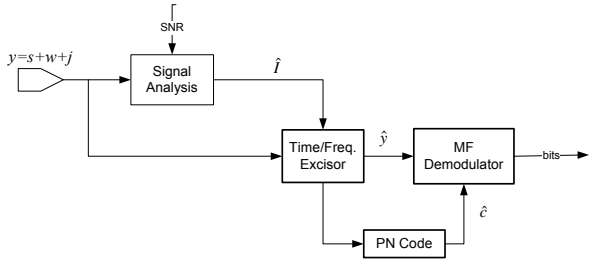

Fig. 1. CARS architecture

With this definition and normalization of the noise power, SNR takes on the usual meaning of Signal-to-Noise Ratio (SNR) and JSR is the Jammer-to-Signal power Ratio (JSR). We introduce some general notation that will be used throughout the paper. We denote by $\hat{y}$, the received signal vector resulting after applying an AJ processing algorithm. The spreading code that is adapted to the excision process is denoted $\hat{c}$. We utilize a simple matched-filter (MF) receiver in this work, whose operation is described by $\Re\{\hat{c}^\dagger \hat{y}\} \underset{b=1}{\overset{b=0}{\gtrless}} 0$, where $()^\dagger$ denotes taking the complex conjugate transpose of a vector.

2.2. CARS architecture

The CARS architecture is shown in Fig. 1. The three key components of a general CARS architecture are

1) Signal analyzer
2) Time/Frequency Excisor
3) Adapted demodulator

The signal analyzer block takes SNR and received baseband signal y as inputs and determines if there is an interference signal present. It continues by estimating the interference characteristics, $\hat{I}$ (see section 2.3 for definition). The signal analyzer block utilizes the fact that the DSSS waveform has a flat, noise-like spectrum. This estimate is provided as an input to the time/frequency excisor (TFE). The TFE removes the interference as best as possible, given the knowledge of the interference class. The outputs of the TFE block are the received signal with interference excised, $\hat{y}$, and corresponding time/frequency excised spreading code, $\hat{c}$, called the *adapted spreading code*. It is well known that an adapted demodulator, which is a matched filter using the adapted spreading code, can provide improved performance, as much as 3 dB in some cases [13]. We refer the reader to [13] for more details and analysis of the adapted demodulator. We describe the signal analyzer in section 3 and the TFE in section 4.

2.3. Interference Classes

For the purpose of configuring the TFE, we define the following two characteristics that will be used to classify the interference type or class:

1) **Bandwidth support**: $B_s \in \{0, 1, \ldots, Q\}$
   This is a measure of the bandwidth occupied by the

interference. In the context of this paper, we define B_s as the maximum number of bands occupied by the interference. The signal bandwidth is partitioned into Q idealized non-overlapping bands. For example, B_s can be estimated by finding the maximum number of channelized radiometer decisions that are simultaneously true.

2) **Time support**: $T_s \in [\Delta T, T]$
where ΔT is the minimum time resolution of the system. T_s is a measure of time occupied by the interference in any band or bands. In the context of this paper, we define T_s as the longest duration of the interference localized in any one of the bands. For example, T_s can be estimated by computing the maximum of the number of consecutive radiometer decisions that are true for each channel.

We provide some example signals and the corresponding values of B_s and T_s to help illustrate:

1) Impulse train interference: $B_s = Q$ and $T_s = \Delta T$
2) Single-tone continuous waveform (CW) interference: $B_s = 1$ and $T_s = T$
3) Multiple-tone CW interference: $B_s = N_j$ and $T_s = T$, where N_j tones are in different bands
4) Frequency-hop interference: $B_s = 1$ and $T_s = T/N_j$, where N_j tones appear one at a time for duration T_s
5) Linear chirp CW interference: $B_s = 1$ and $T_s = T/Q$

The objective of the signal analyzer is to provide accurate estimates of B_s and T_s. It is sometimes useful to quantize these estimates. In the next section, we will use T_s to configure the FFT length, and although not done in this paper, one can suggest rounding the estimates to the closest powers of two. We find it useful to quantize B_s to a binary-valued variable $W(B_s)$, which if true indicates that the interference signal is wideband. We denote the pair $(W(B_s), T_s)$ by I and their estimates $(\hat{W}(B_s), \hat{T}_s)$ by $\hat{I}$.

2.4. Methodology for setting thresholds

In this paper, there are various thresholding (binary hypothesis tests) operations on computed energy observations that need to be performed for both signal analysis and excision purposes. We use a simple methodology for setting these thresholds, parameterized by a False Alarm Rate (FAR) and SNR. The threshold, τ, is determined as a function of the SNR and FAR, α by the following equation (based on Gaussian approximation [14]):

$$\tau = Q^{-1}(\alpha)\sigma_{\text{sn}} + \mu_{\text{sn}} \tag{1}$$

where $Q^{-1}()$ is the inverse Q-function (Gaussian tail probability), σ^2_{sn}, is given by

$$\sigma^2_{\text{sn}} = 4TB + 8\text{SNR}$$

and μ_{sn} is given by

$$\mu_{\text{sn}} = 2TB + 2\text{SNR}$$

where by a slight abuse of notation, $2TB$ is the number of degrees-of-freedom of the signal whose energy is being measured/thresholded. For example, let W represent the complete bandwidth of the system. If we bandpass filter the signal with a filter whose bandwidth is some fraction of W, say $B = \frac{W}{KQ}$ and the number of discrete-time samples (sample rate is W) used in the computation of the energy value is M, then the number of degrees-of-freedom is computed as

$$2TB = 2\frac{M}{W}\frac{W}{KQ} = 2\frac{M}{KQ}$$

3. SIGNAL ANALYZER

The block diagram of the signal analyzer is shown in Fig. 2. The signal to be analyzed is filtered into different bands, and the energy of the filtered output is measured and then further processed to determine the interference class. In the literature, the structure that consists of a bandpass filter followed by an energy measurement and a decision device is known as a *channelized radiometer* and has been used to detect frequency-hopping spread spectrum (FHSS) signals [15]. In Fig. 2, we call a *wideband radiometer* one that measures the energy of the whole band (i.e., without any bandpass filter in front).

There are many possible alternatives for implementing a channelized radiometer, however, in this paper we utilize, for its simplicity, a digital resonator filter bank [16]. The block diagram of a single channelized radiometer is shown in Fig. 3, where the energy measurement is averaged over a moving window of length M. A large value of M provides averaging over several noise samples and reduces the variance of the energy measurements, but M also determines the minimum time resolution. This can be seen, for example, when an impulse is input into the energy-averaging block, the result is a constant output that lasts for M samples.

The output of the energy-averaging block is compared to a threshold that is set by choosing a FAR and knowledge of SNR using 1. The results of the thresholding operation, the binary decisions $d_i(n)$, are further processed for interference classification, where $0 \le i \le Q$ and $i = 0$ is reserved for the wideband radiometer decision. The on cadences of the interference are computed (by counting runs of decisions) for all channels. We denote the maximum on-time estimate for channel i as $\hat{T}_{\text{ON}}(i)$, where $0 \le i \le Q$. Again, $\hat{T}_{\text{ON}}(0)$ corresponds to the maximum on-time for the wideband radiometer.

3.1. Estimating bandwidth and time support of interference

There are several ways to classify interference as *wideband*. We describe one such method. Let us compute a measure that gives an idea of frequency support of the interference at any sample instant $0 \le n \le KN - 1$, as $\hat{B}_s(n)$:

$$\hat{B}_s(n) = \sum_{i=1}^{Q} d_i(n)$$

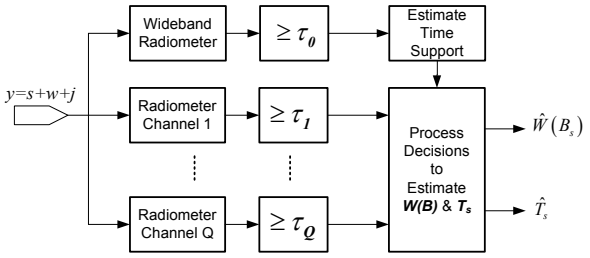

Fig. 2. Signal analyzer

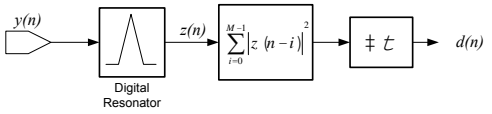

Fig. 3. Discrete-time version of channelized radiometer

From $\hat{B}_s(n)$, we can compute maximum instantaneous frequency support over all $0 \leq n \leq KN-1$, $\hat{B}_s = \max(\hat{B}_s(n))$. Consistent with the description in section 2.3, $\hat{B}_s \in \{0, 1, \ldots, Q\}$. The following rule is used to estimate the binary variable $W(B_s)$:

$$\hat{W}(B_s) = \begin{cases} 1 & \text{if } (\hat{B}_s \geq N_{\mathrm{WB}}) \ \wedge \ (\hat{T}_{\mathrm{ON}}(0) \leq N_{\mathrm{FFT,min}}); \\ 0 & \text{otherwise.} \end{cases}$$

where N_{WB} is a design parameter that represents how many channels must be active simultaneously and $N_{\mathrm{FFT,min}}$ is the minimum FFT length. If $\hat{W}(B_s) = 1$, then an estimate of time support is $\hat{T}_s = \hat{T}_{\mathrm{ON}}(0)$. If $\hat{W}(B_s) = 0$, then an estimate of time support is $\hat{T}_s = \max \hat{T}_{\mathrm{ON}}(i)$, where $1 \leq i \leq Q$.

4. TIME/FREQUENCY EXCISOR (TFE)

If interference is detected to be present, the TFE is used to remove it. The TFE consists of two separate excision methods: a) time (only) excisor b) FFT-based excisor. As shown in Fig. 4, the time excisor is called when the interference is determined to be *wideband* and has a *short duration*. In this paper, the interference has a *short duration* when:

$$N_{\hat{T}_s} \leq N_{\mathrm{FFT,min}}$$

where $N_{\hat{T}_s}$, is the number of discrete-time samples that correspond to $\hat{T}_s$, and $N_{\mathrm{FFT,min}}$ is a design parameter that corresponds to the minimum FFT length for the FFT excisor, which is discussed next. Time excision occurs on a sample-by-sample basis. If the power of a sample exceeds a threshold τ_{TIME} (computed by setting α_{TIME} and using (1)), that sample is excised (or set to zero). The FFT-based excisor is shown in Fig. 5. Each branch operates on a block of N_{FFT} samples. The number of parallel branches depends on the overlap ratio. For example, for an overlap ratio, $\mathrm{OV} = 50\%$, we will have two parallel branches and the number of overlapped samples, $N_{\mathrm{OV}} = \lfloor N_{\mathrm{FFT}} \mathrm{OV} \rfloor$. The block of samples are first windowed (using a suitable window function, for example, Hamming or Gaussian) and then

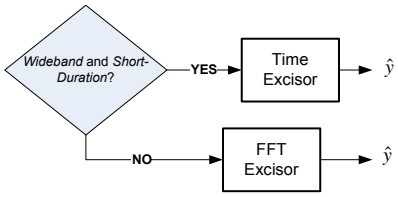

Fig. 4. Time or Time-Frequency excision?

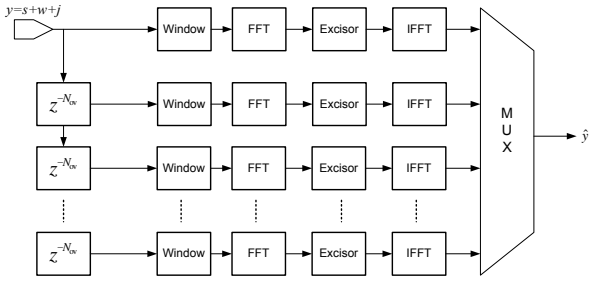

Fig. 5. FFT excisor architecture

TABLE I
PARAMETER VALUES USED IN NUMERICAL EXAMPLE

Parameter Name	Symbol	Value
Samples/chip	K	5
Num. of radiometer channels	Q	16
Num. samples for energy averaging	M	40
Wideband classification parameter	N_{WB}	11
FATS FFT length (samples)	$N_{\mathrm{FFT,FATS}}$	256
Window type		Hamming
Overlap ratio	OV	50%
Min. FFT length	$N_{\mathrm{FFT,min}}$	128
Max. FFT length	$N_{\mathrm{FFT,max}}$	1024
FAR for signal analyzer	α_{SA}	0.01
FAR for FFT excisor	α_{FFT}	0.05
FAR for time excisor	α_{TIME}	0.001

followed by the FFT. The power in each bin is compared to a threshold, τ_{FFT} (computed by setting α_{FFT} and using (1)) and excised if the threshold is exceeded. The excised bin can be set to different values. For example, [7] suggests that setting the excised bins to the background noise level results in an improved performance. In this paper, for simplicity, we set excised bins to zero.

5. SIMULATION EXAMPLE

5.1. Simulation setup

Our simulations use the GPS C/A code (PRN1) as the spreading code, with number of chips $N = 1023$. BPSK modulation is assumed and the symbol (bit) time is assumed to match the code period, which is 1 ms. Unless stated otherwise, the parameters used in the simulation are given in Table I.

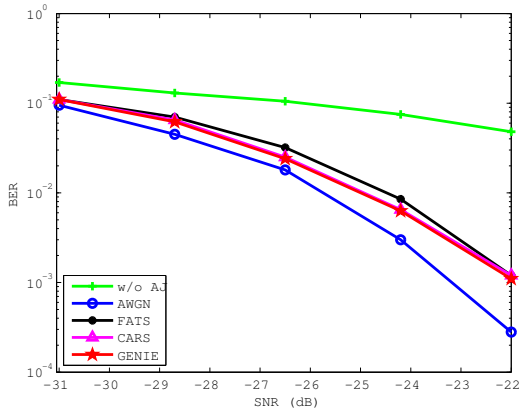

Fig. 6. BER vs. SNR: linear chirp interference at 40 dB JSR. All three AJ schemes—GENIE, CARS, and FATS—exhibit similar performance.

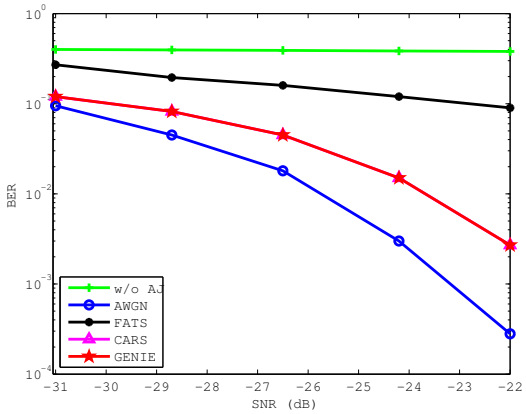

Fig. 7. BER vs. SNR: Eight-tone interference at 40 dB JSR. FATS performs poorly when compared to the CARS approach. Note that CARS performance is indistinguishable from GENIE.

5.2. GENIE and FATS schemes

It is to be noted that all AJ schemes in this paper—namely, FATS, GENIE and CARS—utilize the adapted demodulator as described in [13]. FATS is the fixed AJ scheme and hence is oblivious to the interference character, and thus the FFT excisor is always configured at a fixed length $N_{\text{FFT,FATS}}$. The GENIE method assumes perfect knowledge about the interference and is basically the CARS approach without the possibility of estimation error. For the linear chirp interference, GENIE sets time support as $T_s = \sqrt{\frac{1}{\dot{f}_i}}$, where $\dot{f}_i$ is the derivative of the instantaneous frequency with respect to time. This result is obtained by solving $\dot{f}_i T_s = \frac{1}{T_s}$. Intuitively speaking, for a very slow-changing chirp interference, it is desirable to have a larger frequency resolution.

5.3. BER vs. SNR performance

Figures 6, 7, and 8, show BER vs. SNR performance of all the AJ schemes for three different types of interference. It is noticed that for the linear chirp interference in Fig. 6, all AJ schemes perform more or less similarly, with a small advantage for the CARS approach. In Fig. 7 and eight *tones* of equal power, uniformly spaced over signal bandwidth, we see the superior performance of the CARS approach. In FATS, due to the relatively smaller frequency resolution, a large part of the signal gets excised. In Fig. 8, sixteen uniformly spaced, discrete *impulses* of equal power appear to have little or no impact on the BER of the CARS architecture, which seems to recognize the interference type and excises in time. In all cases, the high JSR of 40 dB seems to render the system without AJ practically useless. We note that the processing (spreading) gain for this DSSS system is $10\log_{10}(1023)$, which is about 30 dB.

5.4. Performance at different JSRs

We are interested in knowing the performance of the CARS approach at various JSRs. Is the estimator able to correctly classify the interference type and indicate what the BER performance is ? Figure 9 shows the BER vs. JSR performance

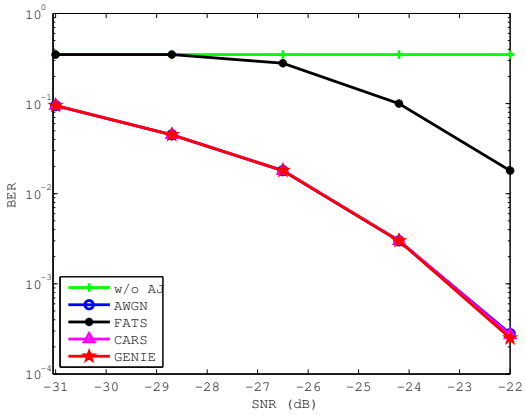

Fig. 8. BER vs. SNR: Sixteen-impulse interference at 40 dB JSR. AWGN, CARS, and GENIE performances are indistinguishable from each other.

at an SNR of -22 dB for a sixteen-impulse interference. We can see that there is a range of JSRs for which the CARS estimation is susceptible to incorrectly determining the interference type, as evidenced by the GENIE performance close to the AWGN or no interference case. In Fig. 10, we show the BER vs. JSR performance subject to a four-tone interference. Note that GENIE performs better than all other AJ schemes and that there is a region of JSR from around 10 to 20 dB where not performing any AJ is actually better than CARS or FATS. This is due to the processing gain of the DSSS scheme. However, as JSR increases, the CARS scheme becomes identical to the GENIE scheme. In both interference cases, the CARS approach provides a way to operate at reasonably good BER performance in a high-JSR environment and provides a considerable improvement over the FATS approach.

6. Conclusion

In this paper, we introduced a novel Cognitive Antijam Receiver System (CARS) approach whereby the antijam (AJ) signal processing and the receiver signal processing

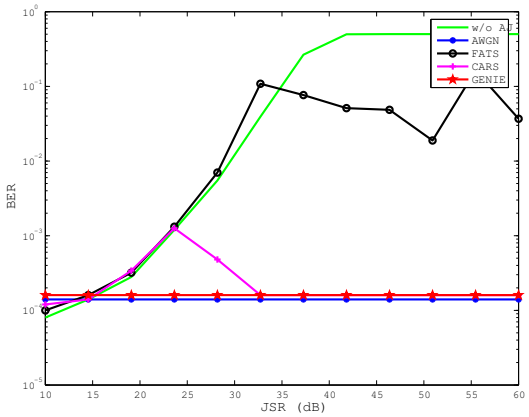

Fig. 9. BER vs. JSR: Sixteen-impulse interference at -22 dB SNR. CARS performs as well as GENIE and AWGN for most JSR, and outperforms FATS.

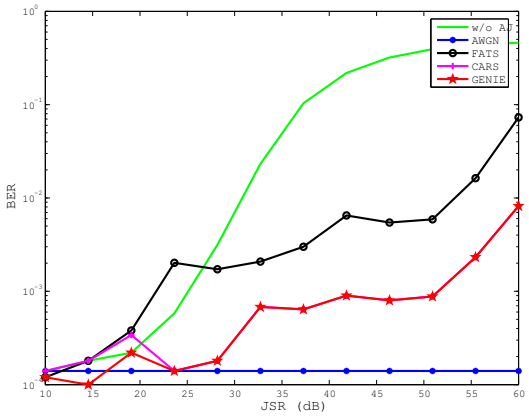

Fig. 10. BER vs. JSR: Four-tone interference at -22 dB SNR. CARS performs as well as GENIE for most JSR, and outperforms FATS.

are jointly adapted to more effectively mitigate interference. A representative CARS architecture was employed that consisted of an interference estimator consisting of a bank of channelized radiometers, decision logic, a time and time-frequency jammer excision block based on the FFT algorithm, and a demodulator that is adapted to the measured jammer characteristics. We demonstrated the relative performance of the CARS architecture as compared to conventional FATS approaches when applied to a DSSS receiver. We find that the FATS approach does not provide adequate performance when compared to the CARS approach. This advantage is observed even when the interference is very simple, like impulses or multiple tones. The CARS approach, by virtue of its adaptability (cognition), is suitable for mitigation of various types of interference.

Further work, currently in progress, involves determining optimum values for the parameters listed in Table I. An important question is how to determine the optimal time support and excision strategy for more complex interferer patterns that are combinations of different interferers. In this paper, we have considered two classes of basis functions (discrete sample basis and parameterized DFT basis). Future work will consider basis functions from the fractional Fourier transform family since these are better equipped to handle chirp-like interference.

REFERENCES

[1] J. Laster and J. Reed, "Interference rejection in digital wireless communications," *IEEE Signal Processing Mag.*, vol. 14, no. 3, pp. 37–62, May 1997.

[2] L. Milstein, "Interference rejection techniques in spread spectrum communications," *Proc. IEEE*, vol. 76, no. 6, pp. 657–671, Jun 1988.

[3] J. Ketchum and J. Proakis, "Adaptive algorithms for estimating and suppressing narrow-band interference in PN spread-spectrum systems," *IEEE Trans. Commun.*, vol. 30, no. 5, pp. 913–924, May 1982.

[4] J. W. Choi and N. I. Cho, "Suppression of narrow-band interference in DS-Spread spectrum systems using adaptive IIR Notch filter," *Signal Process.*, vol. 82, no. 12, pp. 2003–2013, 2002.

[5] G. Gelli, L. Paura, and A. Tulino, "Cyclostationarity-based filtering for narrowband interference suppression in direct-sequence spread-spectrum systems," *IEEE J. Select. Areas Commun.*, vol. 16, no. 9, pp. 1747–1755, Dec 1998.

[6] M. Amin, "Interference mitigation in spread spectrum communication systems using time-frequency distributions," *IEEE Trans. Signal Processing*, vol. 45, no. 1, pp. 90–101, Jan 1997.

[7] R. DiPietro, "An FFT based technique for suppressing narrow-band interference in PN spread spectrum communications systems," *International Conference on Acoustics, Speech, and Signal Processing*, pp. 1360–1363 vol. 2, May 1989.

[8] J. Young and J. Lehnert, "Analysis of DFT-based frequency excision algorithms for direct-sequence spread-spectrum communications," *IEEE Trans. Commun.*, vol. 46, no. 8, pp. 1076–1087, Aug 1998.

[9] P. Capozza, B. Holland, T. Hopkinson, and R. Landrau, "A single-chip narrow-band frequency-domain excisor for a Global Positioning System (GPS) receiver," *IEEE J. Solid-State Circuits*, vol. 35, no. 3, pp. 401–411, Mar 2000.

[10] Y. Wei and G. Bi, "Broadband interference suppression in DSSS system with modifed discrete chirp fourier transform," *Signal Processing*, vol. 84, pp. 1749–1758, 2004.

[11] M. Tazebay and A. Akansu, "Adaptive subband transforms in time-frequency excisers for DSSS communications systems," *IEEE Trans. Signal Processing*, vol. 43, no. 11, pp. 2776–2782, Nov 1995.

[12] S. Aromaa, P. Henttu, and M. Juntti, "Transform-selective interference suppression algorithm for spread-spectrum communications," *IEEE Signal Processing Lett.*, vol. 12, no. 1, pp. 49–51, Jan 2005.

[13] S. Sandberg, "Adapted demodulation for spread-spectrum receivers which employ transform-domain interference excision," *IEEE Trans. Commun.*, vol. 43, no. 9, pp. 2502–2510, Sep 1995.

[14] R. Mills and G. Prescott, "A comparison of various radiometer detection models," *IEEE Trans. Aerosp. Electron. Syst.*, vol. 32, no. 1, pp. 467–473, Jan 1996.

[15] L. Miller, J. Lee, and D. Torrieri, "Frequency-hopping signal detection using partial band coverage," *IEEE Trans. Aerosp. Electron. Syst.*, vol. 29, no. 2, pp. 540–553, Apr 1993.

[16] M. Padmanabhan and K. Martin, "Resonator-based filter-banks for frequency-domain applications," *IEEE Trans. Circuits Syst.*, vol. 38, no. 10, pp. 1145–1159, Oct 1991.